# EFFECT OF TIDAL FLUCTUATIONS ON TRANSIENT DISPERSION OF SIMULATED CONTAMINANT CONCENTRATIONS IN A COASTAL AQUIFER

By I. La Licata
ivana.lalicata@polimi.it

**Index**

# 1 PREFACE

When dealing with exploitation, restoration and management of fresh groundwater in coastal aquifers the key issue is saltwater intrusion.
Coastal aquifer serves as major sources for freshwater supply in many countries around the world and many coastal areas are also heavily urbanized, a fact that makes the need for freshwater even more acute. Coastal aquifers are highly sensitive to disturbance and inappropriate management may lead to its destruction as a source for freshwater much earlier than other aquifers which are not connected to the sea.

As known saltwater intrusion is a natural phenomenon which occurs in every coastal aquifer. It consists of shoreward movement of water from sea or ocean into confined or unconfined coastal aquifers and subsequent displacement of fresh water. Sea water is denser, and for this reason it moves under freshwater forming a wedge progressing into the land.
The position of saltwater wedge under freshwater is capital for the management of a coastal aquifer and for this reason lot of studies have been conducted.

# 2 BRIEF THEORY OF SALTWATER INTRUSION

*Ghyben* (1888) and *Herzberg* (1901) firstly formulated a valid theory about the phenomenon of saltwater intrusion and found a useful relation to describe the shape and position of fresh water-saltwater interface in coastal aquifers.
Referring to figure 1 they formulated the relation

$$h_s = \frac{\gamma_f}{\gamma_s - \gamma_f} h_f = \delta h_f \qquad \textbf{(1)}$$

where $h_s$ = sea level head above point A, $h_f$ = fresh water head above point A respect mean sea level, $\gamma_s$ = saltwater density (1025 kg/m$^3$), $\gamma_d$ = fresh water density (1000 kg/m$^3$).

The constant of proportionality $\delta = \frac{\gamma_d}{\gamma_s - \gamma_d}$ ranges between 33 and 50, commonly $\delta = 40$; this means that the depth $h_s$ of the interface below sea level, is about 40 times the height of water table above mean sea level ($h_f$).

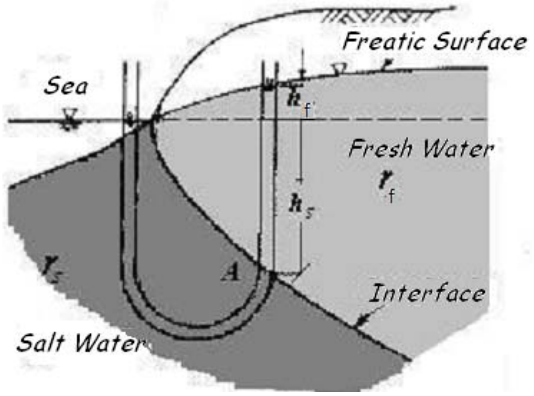


**Figure 1 – Piezometers located above and below the freshwater-saltwater interface showing the equilibrium of columns filled with different density water (from BEAR J.)**

The Ghyben-Herzberg theory is based on some restrictive hypothesis so De Wiest (1965) introduced the concept of *true environmental head* ($h_a$) which is the water level, measured from mean sea level, in a well filled by different density waters (water level in a real well screened over its entire depth) as shown in figure 2. This level is interesting because it is directly measurable.
In this case the pressure at depth $\zeta_3$ can be calculated as:

$$(h_s - \zeta_3)\gamma_s = (h_a + \zeta_1)\gamma_d + \int_{\zeta_1}^{\zeta_2} \gamma(z)dz + (\zeta_3 - \zeta_2)\gamma_s \qquad \textbf{(2)}$$

where $\gamma(z)$ is the specific weight of mixed water in the transition zone (function of $\zeta$) at

depth z. This relation accounts for the thickness of the transition zone.

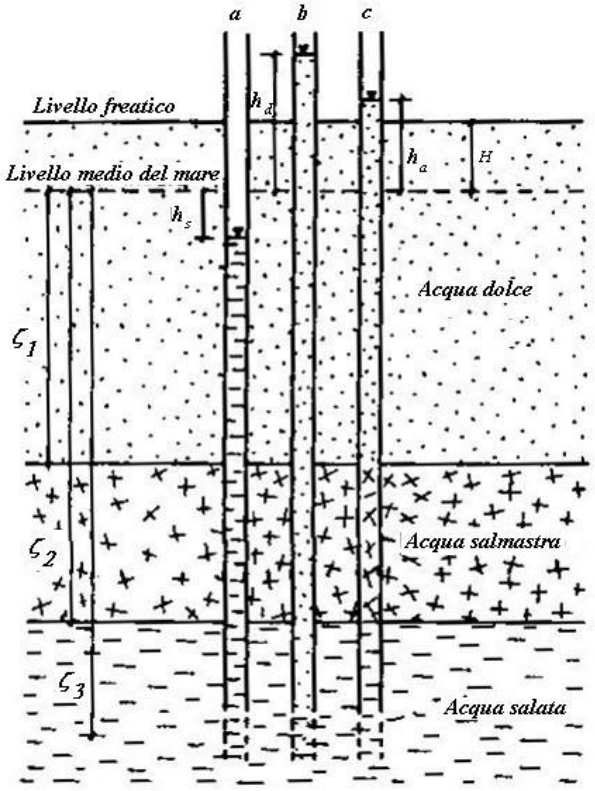


**Figure 2 – a) punctual water level, $h_s$; b) freshwater head, $h_d$; c) environmental or local head, $h_a$**

**(from CUSTODIO E., LLAMAS M.R.)**

# 3 MATHEMATICAL MODELING: TIDE AND TRANSIENT DISPERSION

The problem in studying saltwater intrusion is that some relations are very simple, based on really simplifying assumptions (as Ghyben-Herzberg's), and can be used to have just a qualitative indication about the position of saltwater into the aquifer; others are too complicated and need to be applied lot of parameters that are often difficult to know (as De Wiest's).

For this reason, the use of computer codes able to solve the equations of density-dependent flow and transport has become more and more common. Today, all the studies about saltwater intrusion and coastal aquifers are conducted with the aid of programs like Seawat2000 (finite differences) or Feflow (finite elements), which are two of the most used codes worldwide, and saltwater intrusion models are very common by now.

But simulation of contaminant transport in coastal aquifers is intrinsically complex and computationally expensive because of the complex flow patterns that develop when freshwater mixes with saline groundwater. Because of the density contrast, seawater intrudes landward below freshwater and a diffuse transition zone occurs between these two different fluids. The extent of saltwater intrusion is affected by a large number of physical and hydraulic parameters, such as recharge, hydraulic conductivity and mixing properties. The location and shape of the transition zone influences groundwater flow direction and velocity. Correspondingly, contaminant migration in groundwater is also affected by the characteristics of the transition zone between freshwater and saltwater. An additional complication in simulating contaminant transport in coastal aquifers is the confounding effect of tides which necessitates the use of a short time step, resulting in substantial computational effort (Volker et al. 1998).

Goode and Konikow (1990) compared transport in transient flow fields with that in steady state flow fields having equivalent average fluxes and flow directions, and they found that flow transients, which change the plume migration direction, cause an apparent increase in dispersion. Thus they defined apparent dispersivities as "those values that yield the best match or calibration of the solute transport model under steady state flow conditions to a plume that developed under transient flow conditions". Goode and Konikow independently derived apparent dispersivity expressions similar to those presented by Kinzelbach and Ackerer (1986)

that fitted an observed plume using two models: one model assumed transient flow in response to seasonal fluctuations, the other model assumed steady state flow and used a different value of longitudinal and transverse dispersivity. The relations between apparent and true dispersivities depend on the angle of deviation of the velocity vector from the mean and the ratio of transverse to longitudinal dispersivity.
The concept of transient dispersion is used in this work to test the hypothesis that the effects of tidal mixing can be included in a model with a constant ocean stage boundary by increasing the aquifer dispersivity value.

The purpose of this work is to investigate the influence of tidal variation on solute transport where contaminants reach the freshwater-saltwater transition zone and discharge into the ocean. This is accomplished using simulations based on a simple two-dimensional cross-sectional model that explicitly represents coastal groundwater flow within the freshwater and saltwater transition zone. Simulations that neglected (No Tide) and included (Tide) a tidally fluctuating ocean boundary were compared with the aim to analyze the influence of tidal variation on contaminant behaviour and mass flux toward the sea. Steady state simulations with spatially varying dispersivity values (transient dispersion) were run to improve the representation of mechanical dispersion attributed to hydraulic transients and to evaluate if increasing dispersivity could approximate the transient phenomenon in a steady-flow model. So the influence of transient dispersion on the concentration distribution in a variable-density flow and transport model was investigated.
The Seawat computer program (Langevin et al. 2003; Langevin and Guo 2006) was used for the analyses.

## 3.1 MODEL DESCRIPTION

Groundwater flow and transport simulations were run using a two-dimensional cross-section model (Fig. 3) in which active cells were assigned properties similar to those of a phreatic coastal aquifer located near a coastal refinery in central Italy. The model is based on simulations reported by La Licata et al. (2007; 2008). The parameters assigned to the model are shown in Table 1 and are based on general knowledge, field data, and results from prior studies (Alberti *et al.* 2006). The following linear relation between fluid density ($\rho$) and total dissolved solids concentration (C), referred to here as salinity concentration, was used (Guo and Langevin, 2002): $\rho = 1000 + 0.714C$.

Except for layer 1 and layer 12, the layer thickness is 0.5m. Groundwater flow in layer 1 is represented as unconfined flow; confined flow is represented in layers 2 through 12. The layer 1 bottom is specified at -0.80 m, which is lower than the lowest expected groundwater level so that complications with drying and rewetting would not be encountered.

**Table 1 Parameters assigned to the model**

| | | | |
|---|---|---|---|
| **Height [m]** | 7.5 | **Number of Model Layers** | 12 |
| **Length [m]** | 500 | **Hydraulic Conductivity [m/s]** | from $5\ 10^{-4}$ to $1\ 10^{-3}$ |
| **Number of Rows** | 1 | **Recharge [m/s]** | $5.55\ 10^{-8}$ |
| **Number of Columns** | 201 | **Porosity** | 0.25 |
| **Column Widths** | (range: 1-10 m) | **Layer thicknesses** | Layer 1: 1.60 m<br>Layers 2-11: 0.5 m<br>Layer 12: 0.275 to 0.975 m |

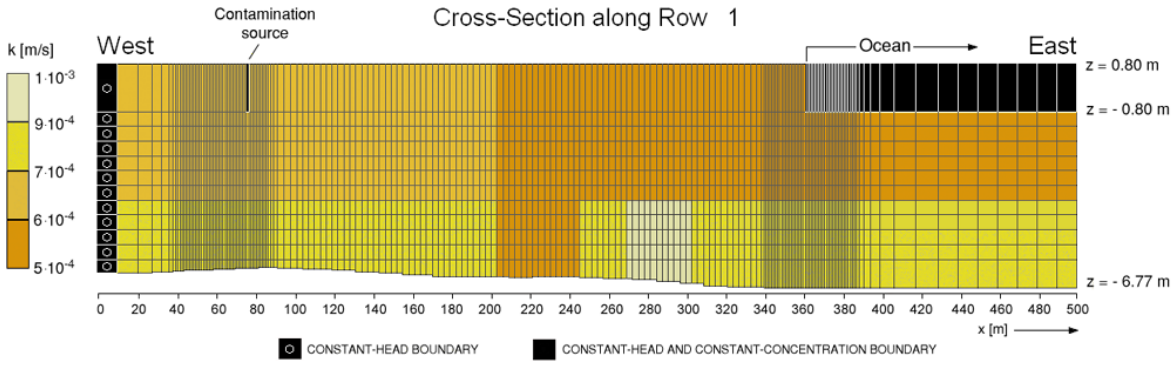


**Figure 3 – Cross section showing model grid, hydraulic conductivity and boundary conditions**

The horizontal grid resolution was refined near the contamination source and near the coastline to ensure accurate transport calculations; the fine resolution and dispersive nature of the problem minimized numerical dispersion, which was periodically evaluated using the higher order, total-variation-diminishing (TVD) scheme in SEAWAT. A constant head equal to 1.25 m was assigned on the western boundary. Constant heads and salinities were assigned in layer 1 to the eastern boundary (Fig. 3) to represent connection of the aquifer to a shallow sea. With this approach, the shallow sea floor is represented as being flat at an elevation of -0.80 m. In the simulation without tides (No Tide) the constant-head boundary representing the sea was set to mean sea level (0 m) and salinity to 35 kg/m3. For Tide, the salinity is the same, but the sea boundary was assigned temporally fluctuating heads to represent tides (Fig.4). A diurnal tidal cycle is simulated in accordance with the relation $h_T = A\sin(\varpi t)$, where hT is the time-varying head (relative to the level 0 m), A is the tidal amplitude, and ⍰ the tidal frequency (1 d-1; period = 1 d). The resulting tidal signal roughly approximates the average tidal signal observed in the northern Adriatic Sea. This daily tidal period is different from tidal characteristics in most coastal areas, which tend to have clear half-day tidal periods. Tide represents a 2-year simulation period using 3-hour stress periods (8 stress periods per tidal cycle).

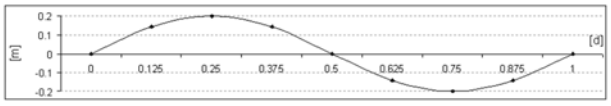


**Figure 4 – Head variations in one tidal cycle**

A contamination source, releasing a hypothetical pollutant, was located at a distance of 75 m from the western border of the model domain. The constant-concentration cell representing the source was assigned an arbitrary concentration value of 1000 kg/m$^3$. The contaminant is simulated as being conservative.

All of the model simulations show the same general pattern of contaminant migration. At the end of the simulation, the distribution of contaminant within the aquifer is at steady state, and the leading edge of the plume has reached the ocean (Fig. 5). As expected, the plume moves toward the freshwater/seawater interface and rises to a shallower part of the section as it reaches the denser water of the transition zone. The contaminant discharges into the ocean through a narrow outflow face near the shoreline.

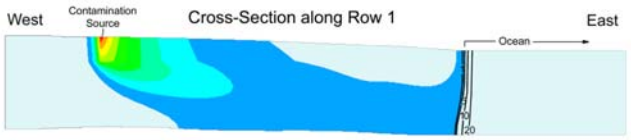


**Figure 5 – Cross section showing simulated contaminant concentrations after two years. Black contours represent salinity isosurfaces**

Contaminant concentrations were compared for *Tide* and *No Tide* simulations to analyze the influence of tidal variations on the contaminant and salinity distributions. Differences are evident in the contaminant and salinity concentrations between *No Tide* and *Tide* at the end of the 2-year simulation period (Figure 6).

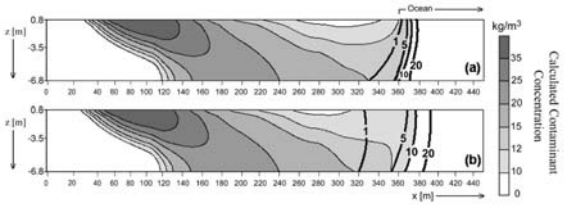


**Figure 6 – Simulated contaminant concentrations and salinities for the case without (a) and with (b) tidal variations. Salinity and contaminant concentrations for the case without tidal variations are shown for the end of the 2-year simulation period. Thick black contours represent salinity isosurfaces in kg/m$^3$.**

The tidally driven hydraulic transients in *Tide* increase the overall mixing resulting in a relatively broader saltwater/freshwater transition zone. The increased mixing in *Tide* also caused contaminant concentrations near the ocean to be lower than for the *No Tide* simulation (Fig. 6). Differences in contaminant concentrations between the two simulations were as high as 15% within the freshwater/saltwater transition zone. This difference is due to the fact that the contaminant mixing patterns are different. This induces a difference in the concentration distribution.

## 3.2 MODEL ANALYSIS - ESTIMATION OF APPARENT DISPERSIVITY

Increasing the dispersivity values near the boundary can be a fast solution to adapt a steady-state model, but calculation of the appropriate value of apparent dispersivity for each cell, based on velocity variation, could improve the approximation of the mechanical dispersion attributed to hydraulic transients. Thus the concept of transient dispersion is used here to test the hypothesis that the effect of tidal mixing can be included in a *No Tide* model by calculating and using apparent dispersivities. Apparent dispersivities for the longitudinal and transverse directions were calculated using the equations presented by Ackerer and Kinzelbach (1986) as shown in the Appendix. The distribution of apparent longitudinal and transverse dispersivity is shown in Figure 7. The equations required the transient velocity variations at each model cell, which were taken from the *Tide* simulation. The calculations shown in the appendix were applied to each cell of the domain to calculate apparent longitudinal and transverse dispersivity values that characterize the velocity variation in that cell during one tidal cycle (8 stress periods). With the exception of the large apparent dispersivities near the upper right corner of the model (which are due to boundary effects), the largest transverse apparent dispersivities are located within the interface between freshwater and saltwater (Figure 7). This is an area where the velocity variation from the average flow direction is the largest and where average flow directions contain a strong vertical component. Apparent longitudinal dispersivities within this same zone are slightly less than the surrounding area.

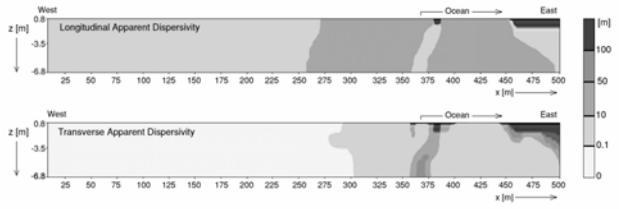


**Figure 7 – Calculated longitudinal and transverse apparent dispersivity**

The velocities used to make the apparent dispersivity calculations are shown for selected cells in Figure 8. The grey arrows represent instantaneous velocities for eight different times within the tidal cycle. The black arrows represent the average groundwater flow velocity, which was calculated from the eight instantaneous velocities. This figure clearly shows the velocity variation that results from tidal fluctuations. For the hydraulic parameters and conditions considered here, velocity variations caused by tidal fluctuations are confined to a 40-m wide zone near the coast. Variations in velocity extend to the bottom of the aquifer.

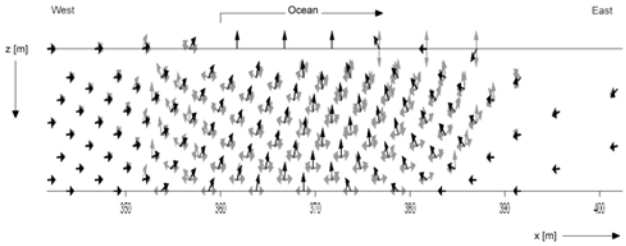


**Figure 8 – Instantaneous velocities for eight stress periods within a single tidal cycle (light grey). Thick black arrows represent average velocity**

The contaminant concentration plume simulated under transient conditions is compared to the plume simulated with steady-state conditions using the apparent dispersivity distribution in Figure 7. The use of apparent dispersivities seems to provide a reasonable approximation of tidal effects. The maximum difference in simulated concentrations is still 15%, but the large differences are confined to areas where contaminant concentrations are relatively low (Fig. 9). For example, the relatively large percent difference at the bottom of the aquifer where x=370 m coincides with the edge of the contaminant plume (Fig. 6b). Although the percent difference is relatively large, the difference in contaminant concentration is less than 17.5 kg/m$^3$.

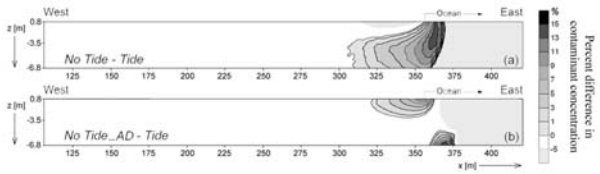


**Figure 9 – Percent difference in contaminant concentration with (a) constant dispersivity and (b) apparent dispersivity**

## 3.3 CONCLUSION

Contaminant transport models require extensive computational resources that can result in lengthy runtimes, especially for those simulations that deal with seawater intrusion and tidal fluctuations. This work presents a comparison of numerical results between contaminant transport simulations with and without tidal effects. Several simulations were performed to investigate the influence of tidal variation on contaminant transport patterns for the situation in which a contaminant in a coastal aquifer migrates through the transition zone and into the ocean.

Simulations reveal that the mixing from tides results in a contaminant and salinity concentration distribution that is more mixed than the distribution for an equivalent steady-state model without tidal effects. This is because of the larger transition zone that develops when tidal effects are included in the simulation. Thus the concentration distribution is different when tide is accounted for because of the different mixing zone. These results could have critical implications for model calibration where erroneous adjustments to parameters may be required to match concentrations in a steady-state model because tides are not explicitly represented. Results indicate that the dispersive mixing effects of tides can be represented in a model that does not explicitly represent tides by increasing the dispersivity value near the ocean.

With the rigorous approach based on the calculation and use of apparent dispersivity values for each cell it's possible to include the

effects of tidal mixing in a steady-state groundwater flow model. The apparent dispersivity distribution created and assigned to the steady-state model using the velocities from a transient model results in similar contaminant and salinity distributions between the two models. The calculated apparent dispersivity correction, therefore, appears to be a practical way to replace tidal effects when calibrating a model. Although this method requires a transient simulation, using the concept of apparent dispersivity could improve model development and calibration because the steady-state contaminant transport model does not require multiple stress periods; therefore, the model simulations require less time to run. Although the concepts presented here were restricted to two dimensions, extension to three dimensions is a logical next step in applying transient dispersion concepts to saltwater intrusion modeling.

# 4 REFERENCES


Ackerer P, Kinzelbach W (1986) Modelisation du transport de contaminant par la méthode de marche au hasard - Influence des variations du champ d'écoulement au cours du temps sur la dispersion. In: Proceeding of Stochastic Approach to Subsurface Flow Symposium, International Association of Hydraulic Research, Montvillargenne, France, v. 1, pp. 517-529.

Alberti L, Francani V, La Licata I, (2006) Hydrogeologic parameters and human activities influence on sea water intrusion at a refinery site. In: International Feflow user conference, Berlin, Germany, 10th-15th Set. 2006.

Bear J., 1979. "*Hydraulics of groundwater"*, MacGraw-Hill, New York.

Bear J., Cheng A. H-D., Sorek S., Ouazar D., Herrera I., 1999 "*Seawater Intrusion in Coastal Aquifers*", Kluwer Academic Publishers.

Custodio E., Llamas M.R., 1996. "*Hidrologia Subterranea",* Omega Ediciones, S.A., Barcelona.
Hubbert M. K., "*The theory of ground-water motion*", J. Geol., 48, 785-944, 1940.

Goode D. J, Konikow L. F (1990) Apparent Dispersion in Transient Groundwater Flow. Water Resour. Res. 26(10), 2339-2351.

Guo W, Langevin C. D (2002) User guide to SEAWAT: a computer program for simulation of three-dimensional variable-density groundwater flow. US Geol. Survey Open File Report 01-434.

La Licata I, Langevin C.D, Dausman A.M (2007) Effect of tidal fluctuations on contaminant transfer to the ocean. In: Sanford W, Langevin C.D, Polemio M and Povinec. P (ed) A new focus on groundwater-seawater interactions. IAHS Publication 312, Oxfordshire, United Kingdom.

La Licata I, Langevin C.D, Dausman A.M, Alberti L (2008) Tidal effects on transient dispersion of simulated contaminant concentrations in coastal aquifers. In: Proceedings of the 20th Salt Water Intrusion Meeting, June 23-27, 2008, Naples, Florida, U.S.A.

Langevin C.D (2003) Simulation of submarine ground water discharge to a marine estuary: Biscayne Bay, Florida. Groundw 41(6):758-771.

Langevin C. D, Guo W (2006) MODFLOW/MT3DMS-Based Simulation of Variable Density Ground Water Flow and Transport. Groundw 44(3):339-351.

Volker R.E, Ataie-Ashtiani B, Lockington D.A (1998) Unconfined coastal aquifer response to sea boundary condition. In: Weaver, Lawrence (ed) Proceedings of International Groundwater Conference, Melbourne, Australia, 8th-13th Feb.

# Appendix: longitudinal and transverse apparent dispersivity calculation

Mass transport of non-reactive chemicals in transient flow fields has been studied previously. Ackerer and Kinzelbach (1986) define the apparent longitudinal and transverse dispersivity resulting from fluctuations in groundwater flow direction as:

$$\alpha_{La} = \alpha_L \frac{\overline{V_L^2}}{V\overline{V_L}} + \alpha_T \frac{\overline{V_T^2}}{V\overline{V_L}}$$

$$\alpha_{Ta} = \alpha_T \frac{\overline{V_L^2}}{V\overline{V_L}} + \alpha_L \frac{\overline{V_T^2}}{V\overline{V_L}} \quad \textbf{(A1)}$$

where $\alpha_L$ and $\alpha_T$ are the true longitudinal and transverse dispersivities [L] respectively, V is the groundwater velocity and $V_L$ and $V_T$ [$LT^{-1}$] are its components in the mean flow and transverse directions, respectively, with overbars indicating time averages.

Here velocities of one tidal cycle simulation along x and z direction were taken from each cell of the domain in *Tide* model.

The following calculations were applied to each cell to calculate apparent longitudinal and transverse dispersivity values that characterize the velocity variation in that cell during one tidal cycle (*n* stress periods). Subscript *i* in calculations refers to stress periods (1, … *n*).

From the extracted $Vx_i$ and $Vz_i$ [$LT^{-1}$] velocities, the mean flow velocity $V$ [$LT^{-1}$] was calculated for the whole tidal cycle:

$$V = \frac{\left(\sum_{i=1}^{8} V_i\right)}{n} \quad \textbf{(A2)}$$

where

$$V_i = \sqrt{Vx_i^2 + Vz_i^2} \quad \textbf{(A3)}$$

is the velocity [$LT^{-1}$] for the $i^{th}$ stress period.

Then for each stress period the flow direction $\vartheta_i$ [°] (i.e. the angle relative to the horizontal) was determined:

$$\vartheta_i = \arctan\left(\frac{Vz_i}{Vx_i}\right) \quad when\ Vx_i \geq 0$$

$$\vartheta_i = \arctan\left(\frac{Vz_i}{Vx_i}\right) + 180° \quad when\ Vx_i < 0 \quad \textbf{(A4)}$$

and the mean flow direction $\vartheta$ [°] was calculated as:

$$\vartheta = \frac{\left(\sum_{j=1}^{8} \vartheta_i\right)}{n} \quad \textbf{(A5)}$$

The component of velocity in the mean flow direction ($V_{Li}$) and the component of velocity transverse to the mean flow direction ($V_{Ti}$) were calculated for each stress period:

$$V_{Li} = V_i \cdot \cos(\Delta\vartheta)$$

$$V_{Ti} = V_i \cdot \sin(\Delta\vartheta) \quad \textbf{(A6)}$$

where

$$\Delta\vartheta = \vartheta_i - \vartheta \quad \textbf{(A7)}$$

represents the deviation of the i$^{th}$ velocity from the mean flow direction [°].
Apparent longitudinal and transverse dispersivity values, $\alpha_{La}$ and $\alpha_{Ta}$ [L], were finally calculated from equations A1 where

$$\overline{V_L} = \frac{\left(\sum_{i=1}^{8} V_{Li}\right)}{n} \quad \textbf{(A8)}$$

and

$$\overline{V_L^2} = \frac{\left(\sum_{i=1}^{8} V_{Li}^2\right)}{n} \quad \textbf{(A9)}$$

$$\overline{V_T^2} = \frac{\left(\sum_{i=1}^{8} V_{Ti}^2\right)}{n}$$